Regenerative Therapy 20 (2022) 107–116

Contents lists available at ScienceDirect

Regenerative Therapy

journal homepage: http://www.elsevier.com/locate/reth

Original Article

Human bone marrow mesenchymal stem cell-derived exosomes containing microRNA-425 promote migration, invasion and lung metastasis by down-regulating CPEB1

Guoqiang Wang [a], Xiuli Ji [b], Pan Li [a], Wei Wang [c, *]

[a] Department of Oncology, Binzhou Central Hospital, Binzhou, Shandong 251700, PR China
[b] Department of Respiratory, Jinan Municipal Hospital of Traditional Chinese Medicine, Jinan, Shandong 250012, PR China
[c] School of Medicine, Cheeloo College of Medicine, Shandong University, Jinan, Shandong 250012, PR China

ARTICLE INFO

Article history:
Received 21 January 2022
Received in revised form
24 February 2022
Accepted 17 March 2022

Keywords:
Lung cancer
Human bone marrow mesenchymal stem cell
Exosomes
MicroRNA-425
Cytoplasmic polyadenylation binding protein 1
Epithelial-mesenchymal transition
Migration
Invasion
Metastasis

ABSTRACT

Objective: Bone marrow mesenchymal stem cell-derived exosomes (BMSC-Exos) could mediate the malignancy of tumor cells by transmitting targeted cargo. Therein, this study intends to explore the function of BMSC-Exos transmitting microRNA-425 (miR-425)/cytoplasmic polyadenylation binding protein 1 (CPEB1) in lung cancer growth.
Methods: miR-425 and CPEB1 levels in cancer tissues and cells were measured. BMSCs and their exosomes were collected and identified. After intervention with BMSC-Exos, miR-425 or CPEB1, invasion and migration of A549 and NCI-H1299 cells *in vitro*, and lung metastasis of A549 cells *in vivo* were observed. The relationship between miR-425 and CPEB1 was verified.
Results: miR-425 was highly expressed while CPEB1 was lowly expressed in lung cancer tissues of patients. CPEB1 was the direct target of miR-425. Down-regulating miR-425 or up-regulating CPEB1 decreased cell invasion and migration ability of A549 and NCI-H1299 cells, as well as decreased the number of lung metastasis lesions *in vivo*. After co-culture with BMSC-Exos, A549 and NCI-H1299 cells showed promoted migration and invasion *in vitro* and A549 cells demonstrated increased lung metastasis *in vivo*. Down-regulated miR-425 or up-regulated CPEB1 reversed the promotion of BMSC-Exos on lung cancer cell invasion, migration and lung metastasis.
Conclusion: BMSC-Exos could deliver miR-425 to inhibit CPEB1 expression in lung cancer cells, thereby promoting the malignant biological properties of lung cancer cells and their metastasis *in vivo*.

1. Introduction

Lung cancer is the leading devastating cancer all over the world [1]. Smoking has been proposed to be the overwhelming cause of lung cancer, yet there are also other risk factors, including air pollution, radon, occupational exposure, genetic susceptibility, radiation and diet [2]. It is reported that in China, lung cancer has become the first cause of cancer death in place of liver cancer, and it is estimated by the World Health Organization that by 2025, the annual mortality rate of lung cancer in China is likely to reach 1 million [3]. Evidence has also shown that the overall five-year survival rate of lung cancer is only 12% in men and 7% in women [4]. In the light of the astonishing mortality and unfavorable prognosis, it is very necessary to seek for new ways of lung cancer treatment.

Exosomes refer to extracellular signalosomes which boost eukaryotic intercellular communication under various normal physiological contexts [5]. Evidence has shown that bone marrow mesenchymal stem cell (BMSC)-derived exosomes promote multiple myeloma cell growth and induce drug resistance [6]. MiRNAs are endogenous non-coding small RNAs with 18–25 nucleotides and function in the regulation of specific target gene [7]. As a part of miRNAs, miR-425 has been found to positively function in lung

* Corresponding author. School of Medicine, Cheeloo College of Medicine, Shandong University, No.44 Wenhua West Road, Jinan, Shandong, 250012, PR China.
E-mail address: Wangwei81203@163.com (W. Wang).
Peer review under responsibility of the Japanese Society for Regenerative Medicine.

https://doi.org/10.1016/j.reth.2022.03.007

adenocarcinoma progression through A disintegrin and metalloproteinases 9 modulation [8]. There has also been a study suggesting that in gastric cancer, miR-425-5p modulates cylindromatosis to affect tumor progression [9]. An early report by Fang F et al. has revealed that in hepatocellular carcinoma, miR-425-5p contributes to cell invasion and metastasis via SCAI-mediated dysregulation of various signaling pathways [10]. In fact, human BMSC-derived exosomal miRNAs have been discovered to promote metastasis of lung cancer cells in the hypoxic niche [11]. Cytoplasmic polyadenylation element-binding protein 1 (CPEB1) refers to a kind of sequence-specific RNA-binding protein which can function in the regulation of mRNA polyadenylation and translation and tumor tumorigenesis [12]. A report has shown that decreased CPEB1 results in lung metastasis of breast cancer cells *in vivo* [13]. It is also indicated that in endometrial cancer, CPEB1 elevation constrains cell development and tumor growth while CPEB1 diminution boosts epithelial-mesenchymal transition (EMT), migration and invasion of cancer cells [14]. This study intends to find out the mechanism of BMSC-Exos on lung cancer by modulating miR-425 and CPEB1.

2. Materials and methods

2.1. Ethics statement

The study was approved by the Ethics Committee of School of Medicine, Cheeloo College of Medicine, Shandong University (ethical approval number: KY2014-080) and informed written consents were obtained from all patients. All animal experiments were approved by the Guide for the Care and Use of Laboratory Animal by International Committees (ethical approval number: KY2014-112).

2.2. Experimental subjects

A total of 93 non-small cell lung cancer tissue specimens and corresponding adjacent normal lung tissue specimens were surgically resected in Cheeloo College of Medicine, Shandong University. None of patients had received chemotherapy or radiotherapy before operation. Specimens were confirmed by pathological diagnosis after operation. Among the 93 patients, there were 64 males and 29 females including 56 cases aged $\geq$60 years old and 37 cases aged <60 years old, with an average age of 55.58 $\pm$ 8.93 years old; and 71 cases of squamous cell carcinoma and 22 cases of adenocarcinoma. According to the staging criteria established by Union for International Cancer Control in 1997, 41 cases were in stage I and II and 52 cases in stage III and IV. Based on the degree of histological differentiation, there were 44 cases with low differentiation and 49 cases with moderate and high differentiation, including 58 cases with lymph node metastasis while the other 35 cases without.

2.3. Cell culture

Isolation and culture of human BMSCs: Bone marrow fluid was extracted from healthy donors by bone marrow puncture and anticoagulated by sodium heparin. BMSCs were extracted by density gradient centrifugation combined with whole bone marrow culture method. The bone marrow fluid was diluted with high glucose Dulbecco modified Eagle medium (DMEM) containing 10% fresh fetal bovine serum (FBS) at 1:1, added with 20 mL Ficoll separation medium and centrifuged at 2000 rpm/min for 20 min. After that, the cells with white membrane in the second layer were rinsed with phosphate buffered saline (PBS) and centrifuged at 1000 rpm/min for 10 min (twice). Then, the cells were incubated in 5 mL α-MEM medium containing 10% fresh FBS for 24 h. After that, the medium was replaced with α-MEM with 10% fresh FBS. BMSCs were observed under a microscope (Olympus, Tokyo, Japan) after 3 repeated medium replacement.

Normal human embryonic lung fibroblast HFL1 and A549 lung cancer cells were purchased from Cell Resource Center of Shanghai Institutes for Biological Sciences, Chinese Academy of Sciences (Shanghai, China) while human lung cancer cells (NCI-H1299, NCI-H292) were from ATCC (VA, USA). NCI-H1299 and NCI-H292 cells were cultured in Roswell Park Memorial Institute (RPMI)-1640 complete medium containing 10% FBS, and 1% penicillin/streptomycin while HFL1 cells and A549 cells in Ham's F-12K (Kaighn's) medium containing 10% FBS and 1% penicillin/streptomycin. The cells were passaged every 3 days, and the cells in the logarithmic growth phase were taken for experiments.

2.4. Cell transfection

NCI-H1299 and A549 cells were divided into 6 groups: inhibitor-negative control (NC) group (transfected with miR-425 inhibitor NC), miR-425 inhibitor group (transfected with miR-425 inhibitor), pcDNA-NC group (transfected with pcDNA-empty-vector), pcDNA-CPEB1 group (transfected with pcDNA CPEB1 vector), miR-425 mimic + pcDNA-NC group (transfected with miR-425 mimic and pcDNA-empty-vector) and miR-425 mimic + pcDNA-CPEB1 group (transfected with miR-425 mimic and pcDNA CPEB1).

NCI-H1299 and A549 cells were seeded in 6-well plates and transfected with the oligonucleotides and plasmids (GenePharma, Shanghai, China) by Lipofectamine™ 2000 transfection reagent (Invitrogen, CA, USA). Cells were collected 48 h after transfection for subsequent cell experiments.

2.5. Identification of BMSCs

Immunophenotypes of BMSCs: BMSCs were made into cell suspension (1×10^6 cells/mL), and the cell suspension (100 μL) was incubated with 10 μL CD29-phycoerythrin (PE), CD44-PE, CD90-fluorescein isothiocyanate (FITC), CD34-FITC and CD45-FITC, respectively. A blank control was set. Next, the cells were resuspended in PBS after 5-min centrifugation at 1000 g and detected in a flow cytometer (Miltenyi Biotec, North Rhine-Westphalia, Cologne, Germany).

Adipogenic induction of BMSCs: BMSCs were cultured to full confluence, and treated with adipogenic induction solution (high glucose DMEM, 10% fresh FBS, 20 μg/mL bovine insulin, 1 mmol/L 1-methyl-3-isobutylxanthine, 1 μmol/L dexamethasone and 25 μmol/L indometacin) for 14 d, during which the solution was renewed every 2 d. Ultrapure water was added to the isopropanol to adjust the concentration to 60%, and the oil red O dye was added until it was no longer dissolved. After removing the adipogenic induction solution, BMSCs were fixed in paraformaldehyde for 15 min, and strained with the oil red O dye solution for 10 min, followed by decolorization with isopropyl alcohol and observation under an inverted microscope.

Osteogenic induction of BMSCs: When cells were fully adhered, they were cultured with osteogenic induction solution (high glucose DMEM, 10% fresh FBS, 10-7 mol/L dexamethasone, 50 μg/mL vitamin C and 10 mmol/L β-glycerophosphate) for 21 d with the solution replaced every 2 d. Then 2 g alizarin red was dissolved in 100 mL ultrapure water to adjust the pH to 4.2. After osteogenic induction solution removal, the alizarin red staining solution was added to stain BMSCs for 5 min and BMSCs were observed under an inverted microscope.

2.6. Extraction, identification and labeling of exosomes

Extraction of BMSC-Exo: When cells reached 70–80% confluence, the culture medium was renewed with FBS-free medium, and BMSCs were incubated for another 48 h. Subsequently, the media were collected. After centrifugation at 4 °C (500 g × 10 min, 12000 g × 20 min), the supernatant was filtered with a 0.22 μm filter and ultracentrifuged (100,000 g) for 2 h. Then the precipitates were resuspended in PBS and ultracentrifuged for 2 h again. The final pellet was resuspended in PBS and stored at −80 °C.

Identification of BMSC-Exo: 1. BMSC-Exo suspension was diluted with 10 μL PBS, added to the loaded copper mesh for 1 min, stained with 3% (w/v) sodium phosphotungstate solution for 5 min, washed with ddH_2O and observed with a transmission electron microscope (TEM, Hitachi High-Technologies Corporation, Tokyo, Japan); 2. Western blot was adopted to detect the surface antigen of BMSC-Exo (CD9, CD81, TSG101 and GRP94). 3. Nanoparticle tracking analysis (NTA): BMSC-Exo were diluted with PBS to 3-5 × 10^7 particles/mL and tested by ZetaView PMX 110. ZetaView 8.04.02 SP2. software was adopted for data analysis.

Observation of the uptake of BMSC-Exo by lung cancer cells via PKH26 staining: Freshly extracted BMSC-Exo were supplemented with 1 mL Diluent C. PKH26 dye (1 mM, 4 μL; Sigma Aldrich, MO, USA) was added to 1 mL Diluent C. Next, exosomes were labeled with red fluorescent PKH26 as described previously [15]. After that, the cells were stained by 4′,6-diamidino-2-phenylindole for 10 min, quenched by anti-fluorescence quenching solution and photographed under a fluorescence microscope.

2.7. Cell co-culture

Synthetic inhibitor-NC, miR-425 inhibitor, pcDNA-NC, pcDNA-CPEB1, miR-425 mimic + pcDNA-NC, miR-425 mimic + pcDNA-CPEB1 were transfected into BMSCs. BMSCs after 24-h transfection were co-cultured with lung cancer cells. BMSCs (1 × 10^5) were seeded into the upper side while lung cancer cells (3 × 10^5) into the lower chamber (Transwell chamber with the aperture of 0.4 μm). In addition, the BMSC-Exo group was set with untransfected BMSCs co-cultured with lung cancer cells. The BMSC-Exo + GW4869 group was set with untransfected BMSCs co-cultured with lung cancer cells and added with 5 μM exosome inhibitor GW4869 (HY-19363, MCE, Monmouth Junction, NJ, USA). A control group was set with medium co-cultured with lung cancer cells. Transfected BMSCs were co-cultured with lung cancer cells for 24 h, and then used in subsequent experiments.

2.8. Reverse transcription quantitative polymerase chain reaction (RT-qPCR)

RNA was extracted by Trizol reagent (Invitrogen). Reverse transcription of the extracted RNA was carried out on the PrimeScript RT kit (Promega, Madison, USA). Genes were quantitatively analyzed via SYBR Green Master Mix (Life Technologies, CA, USA). miR-425 expression was quantified by Mir-X™ miRNA TB Green qPCR kit (Takara, Tokyo, Japan). The primer sequences were shown in Supplementary Table 1. Using glyceraldehyde phosphate dehydrogenase (GAPDH) and U6 as internal controls, gene expression was calculated via $2^{-\Delta\Delta Ct}$ method [16].

2.9. Western blot analysis

Total protein was extracted and protein concentration was determined by bicinchoninic acid kit (AmyJet Scientific, Wuhan, Hubei, China). The extracted protein was mixed with the loading buffer, boiled at 95 °C for 10 min and centrifuged, followed by electrophoresis with 10% polyacrylamide gel. Then, the protein sample was transferred into a membrane and blocked in tris-buffered saline with Tween 20 with 5% skim milk for 1 h. Next, primary antibodies CPEB1 (1:1000, Novus Biologicals, Colorado, USA), CD9 (1:100, BD Pharmingen, New Jersey, USA), CD81 (1:200, Santa Cruz Biotechnology, Santa Cruz, CA, USA), TSG101 (1:1000), GRP94 (1:1000, Abcam, MA, USA), and GAPDH (1:1000, Cell Signaling Technology, Beverly, MA, USA) were combined with the protein membrane overnight. Subsequently, the corresponding secondary antibody (1:2000, Abcam) was added into the protein sample, followed by development with chemiluminescent reagent and protein band analysis with ImageJ2x software.

2.10. Scratch test

After 48 h of transfection or 24 h of co-culture, lung cancer cells (1 × 10^5) were added to 24-well plates. After the cells spread over the whole plate, scratches were drawn, and detached cells and cell debris were washed off by sterile PBS. The scratch width was measured at 0 h, and 48 h respectively to calculate the average migration distance.

2.11. Transwell assay

After 48 h of transfection or 24 h of co-culture, Matrigel (100 μL, 50 mg/L) was diluted at 1:40, and added to the upper chamber. Lung cancer cells were resuspended in serum-free medium and the cell suspension (2 × 10^5 cells/mL, 100 μL) was added in the upper chamber while 600 μL medium containing 20% exosome-free FBS in the lower chamber. Incubated for 24 h, the cells were fixed by methanol for 10 min, stained by 1% crystal violet solution and photographed in 8 fields of view under a microscope.

2.12. Lung metastasis assay

Forty five male BABL/c nude mice, 6 weeks old, were acquired from Beijing Vital River Laboratory Animal Technology Co., Ltd. (Beijing, China) and divided into 15 groups with 3 in each group. Cells (stably transfected A549 cells or A549 cells after 24-h co-culture with transfected or untransfected BMSCs) were prepared into cell suspension. The cell suspension was supplemented with serum-medium to 5 × 10^6 cells/mL and injected to the nude mice at 100 μL through the tail vein. After 4 weeks, the mice were euthanized to take out complete lung tissues, including the trachea and bronchus, and lung metastasis was observed. The lung tissues were fixed in 4% paraformaldehyde and prepared to paraffin slices for hematoxylin-eosin (HE) staining.

2.13. Dual luciferase reporter gene assay

The binding site of miR-425 to CPEB1 3′-untranslated regions (3′-UTR) was predicted in the bioinformatics software (http://www.targetscan.org). Luciferase reporter gene assay was performed using the dual luciferase analysis system kit (Promega). The wild type (WT) and mutant (MUT) pmirGLO-CPEB1-3′UTR vector (Guangzhou Yingxin Co., Ltd., Guangzhou, China) contained the miRNA binding sites. Lung cancer cells were co-transfected with the vector with miRNA mimic. After 48 h, passive lysis buffer sample (20 μL) and Luciferase Assay Reagent II (100 μL) were added to cells and absorbance was measured at 580 nm on a microplate reader. Also, Stop&Glo reagent (100 μL) was added into cells and absorbance was read at 460 nm [17].

2.14. Statistical analysis

All data were processed with SPSS 21.0 software (IBM, NY, USA). The measurement data were expressed as mean ± standard deviation. The comparison between the two groups was made by t-test while that among multiple groups by one-way analysis of variance (ANOVA), after which pairwise comparison was performed by Tukey's post-hoc test. Pearson correlation analysis was performed. $P < 0.05$ suggested statistically significant difference.

3. Results

3.1. MiR-425 is up-regulated and CPEB1 is down-regulated in lung cancer tissues of patients

MiR-425 and CPEB1 expression in lung cancer tissues and corresponding adjacent normal tissues was detected by RT-qPCR and Western blot analysis. MiR-425 expression was higher while CPEB1 expression was lower in lung cancer tissues than in adjacent normal tissues (both $P < 0.05$) (Fig. 1A–D).

Pearson correlation analysis between miR-425 and CPEB1 mRNA expression in lung cancer tissues of patients found that miR-425 was negatively correlated with CPEB1 mRNA expression ($P < 0.05$) (Fig. 1E). miR-425 and CPEB1 mRNA in different lung cancer cell lines was also measured, and the results showed that compared with HFL1 cells, miR-425 expression was up-regulated while CPEB1 mRNA expression was down-regulated in lung cancer cells (A549, NCI-H1299 and NCI-H292) (Fig. 1F). A549 and NCI-H1299 cells had the most significant differences in miR-425 and CPEB1 expression from HFL1 cells, thus the two cell lines were used for follow-up studies.

Online prediction found that there was a miR-425 binding site on the 3′UTR of CPEB1 (Fig. 1G). To confirm that, dual luciferase reporter gene assay was conducted and found that co-transfection of miR-425 mimic and CPEB1-WT suppressed the luciferase activity of lung cancer cells (Fig. 1H), while that of CPEB1-MUT and miR-425 mimic had no influence on luciferase activity of lung cancer cells, indicating that CPEB1 was a direct target of miR-425.

3.2. Inhibitory effects of down-regulating miR-425 or up-regulating CPEB1 on lung cancer cell invasion and migration properties in vitro and lung metastasis in vivo

To further explore the effects of miR-425 and CPEB1 on lung cancer cells, A549 and NCI-H1299 cells were transfected with miR-425 inhibitor/mimic, pcDNA-CPEB1 or the relative NC. The

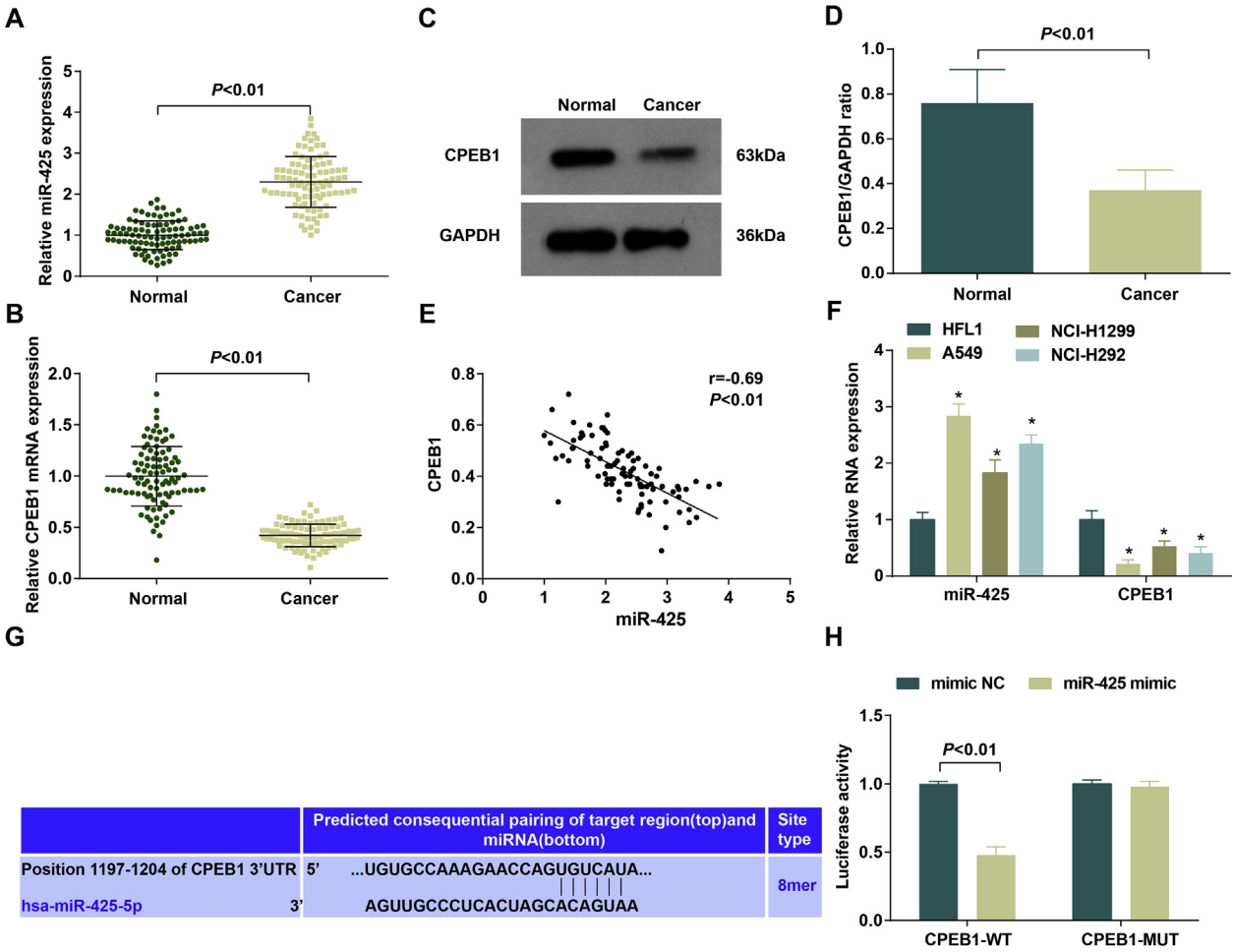

Fig. 1. MiR-425 is up-regulated and CPEB1 is down-regulated in lung cancer tissues; miR-425 targets CPEB1. A. RT-qPCR detection of miR-425 expression in lung cancer tissues (n = 93) and adjacent normal tissues (n = 93); B. RT-qPCR detection of CPEB1 mRNA expression in lung cancer tissues (n = 93) and adjacent normal tissues (n = 93); C-D. Protein bands and protein expression of CPEB1 by Western blot analysis (n = 93); E. Pearson correlation analysis of the relation between miR-425 expression and CPEB1 mRNA expression in lung cancer patients; F. miR-425 and CPEB1 mRNA expression in HFL1 and lung cancer cell lines (A549, NCI-H1299 and NCI-H292); G. Targetscan prediction of the targeting relationship between miR-425 and CPEB1; H. Dual luciferase reporter gene assay validation of the targeting relationship between miR-425 and CPEB1. Data in the figure were expressed by mean ± standard deviation; Comparison between two groups was analyzed by t-test.

results of RT-qPCR and Western blot analysis showed that versus the inhibitor-NC group, the miR-425 inhibitor group demonstrated reduced miR-425 and increased CPEB1 expression (both $P < 0.05$). Relative to the pcDNA-NC group and the miR-425 mimic + pcDNA-NC group, respectively, CPEB1 expression was elevated in the pcDNA-CPEB1 group and the miR-425 mimic + pcDNA-CPEB1 group (both $P < 0.05$) (Fig. 2A and B; Supplementary Figs. 1A and B).

Scratch test and Transwell assay revealed that versus the inhibitor-NC group and the pcDNA-NC group, respectively, suppressed migration and invasion abilities of lung cancer cells were seen in the miR-425 inhibitor group and the pcDNA-CPEB1 group. With respect to the miR-425 mimic + pcDNA-NC group, the miR-425 mimic + pcDNA-CPEB1 group showed decreased cell migration and invasion abilities (all $P < 0.05$) (Fig. 2C–F; Supplementary Figs. 1C–F).

Further exploration of the effects of miR-425 and CPEB1 on lung metastasis *in vivo* was performed by injecting stably transfected A549 into nude mice through the tail vein. HE staining pictured that nuclear aberration, nuclear pyogenic infection, karyokinesis,

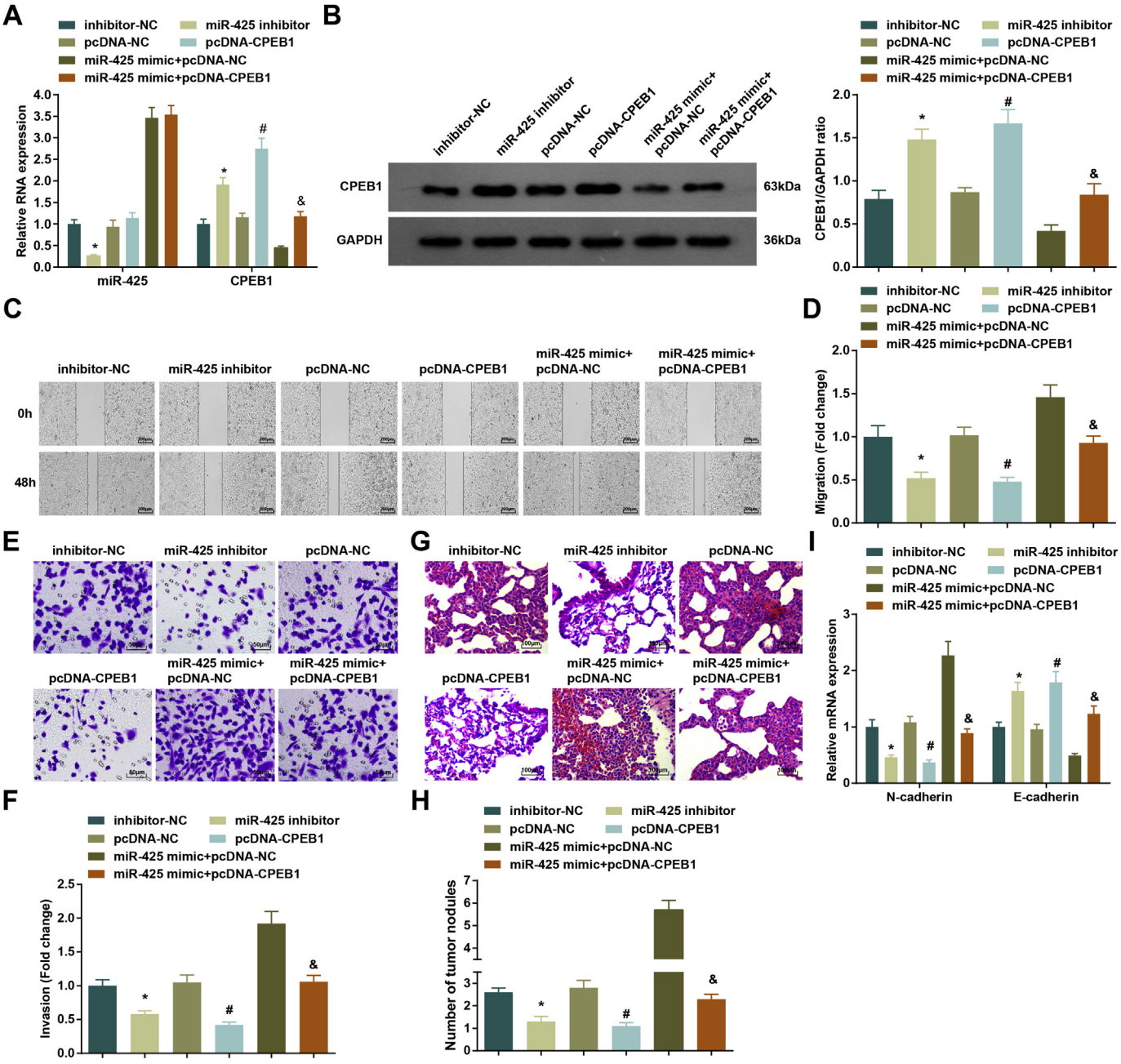

Fig. 2. Down-regulation of miR-425 or up-relation of CPEB1 inhibits A549 cell invasion and metastasis and lung metastasis in nude mice. A. MiR-425 and CPEB1 mRNA expression in A549 cells after transfection detected by RT-qPCR; B. CPEB1 protein expression in A549 cells after transfection detected by Western blot; C-D. Migration of A549 cells after transfection detected by scratch test; E-F. Cell invasion abilities of A549 cells after transfection detected by Transwell assay; G. Stably transfected A549 were injected into nude mice to construct a lung metastasis model, and HE staining observed lung metastasis in tumors of nude mice; H. Number of lung nodules in each group; I. RT-qPCR of N-cadherin and E-cadherin mRNA expression in tumors of nude mice. *$P < 0.05$ compared with the inhibitor-NC group; #$P < 0.05$ compared with the pcDNA-NC group; & $P < 0.05$ compared with the miR-425 mimic + pcDNA-NC group. Data in the figure were expressed by mean ± standard deviation.

abnormal ratio of nuclear and plasma, proliferated nuclei and reduced voids were found in the tumor site in the inhibitor-NC group, pcDNA-NC group, miR-425 mimic + pcDNA-CPEB1 group and miR-425 mimic + pcDNA-NC group. The miR-425 mimic + pcDNA-NC group had the most lung tissue metastatic lesions. The miR-425 inhibitor group and the pcDNA-CPEB1 group were characterized by less lung tissue metastatic lesions in comparison with the inhibitor-NC and the pcDNA-NC groups, respectively (both $P < 0.05$) (Fig. 2G and H).

RT-qPCR was used to detect interstitial marker (N-cadherin) and epithelial mediator (E-cadherin) related to tumor invasion and metastasis in lung tissues of nude mice. It was demonstrated that versus the inhibitor-NC group, pcDNA-NC group, and miR-425 mimic + pcDNA-NC group, respectively, decreased N-cadherin mRNA and increased E-cadherin mRNA expression was found in the miR-425 inhibitor group, pcDNA-CPEB1 group and miR-425 mimic + pcDNA-CPEB1 group (all $P < 0.05$) (Fig. 2I). It was confirmed that suppressing miR-425 or elevating CPEB1 limited invasion and migration of lung cancer cells *in vitro* and lung metastasis *in vivo*.

3.3. BMSCs immunophenotype, and identification of adipogenic and osteogenic induction of BMSCs

After separation of BMSCs, flow cytometry was applied to detect surface antigens of BMSCs. The results showed that CD29 (97.56%), CD44 (92.78%) and CD90 (92.53%) were all positively expressed, while CD34 (1.67%) and CD45 (3.82%) were negatively expressed in BMSCs (Fig. 3A).

Microscopic observation indicated that the morphology of BMSCs cultured to P3 was relatively consistent, showing fibroblast-like shape and adherent growth. There were few impurities around and no cells in other forms (Fig. 3B).

Adipogenic induction of BMSCs suggested that large and round lipid droplets appeared in some cells and these lipid droplets were stained red after oil red O staining (Fig. 3C). Osteogenic induction of BMSCs indicated that some cells showed a shape change from spindle to polygon, and the cell body was enlarged, followed by continuous cell proliferation and overlap. Additionally, there were many nodules stained red by alizarin red solution (Fig. 3D). Osteogenic and adipogenic differentiation of BMSCs reached more than 95%, indicating that BMSCs were successfully isolated.

3.4. Identification of BMSC-Exo

After extraction and purification, BMSC-Exos were identified. The morphology of BMSC-Exo was observed by TEM, which showed that the exosomes were concave oblong or round in shape, with a diameter of 40–100 nm and complete phospholipid bilayer membrane structure (Fig. 4A). Western blot analysis indicated that CD9, CD81 and TSG101 were positively expressed while GRP94 was not expressed in BMSC-Exo (Fig. 4B). The peak size of exosomes detected by ZateView was 76 nm with the particle concentration of

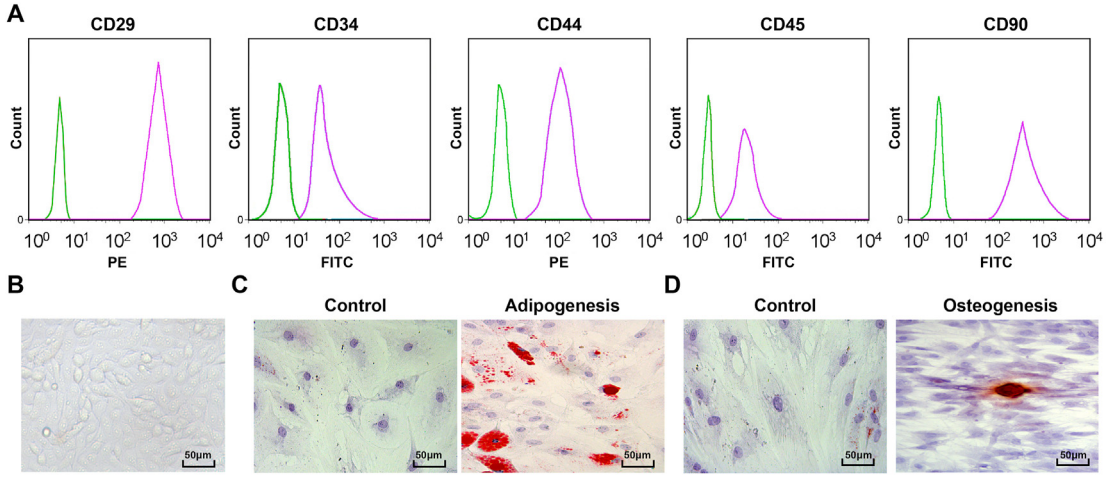

Fig. 3. BMSCs immunophenotype, and identification of adipogenic and osteogenic induction of BMSCs. A. BMSCs surface antigens CD29, CD44, CD90 and non-BMSCs surface antigens CD34 and CD45 detected by flow cytometry; B. BMSCs morphology observed under an inverted microscope; C. BMSCs adipogenic differentiation observed by oil O red staining; D. BMSCs osteogenic differentiation observed by Alizarin Red Staining.

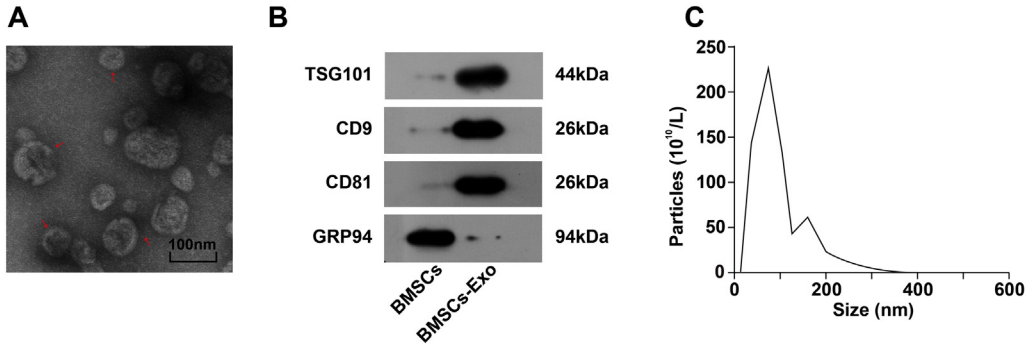

Fig. 4. Identification of BMSC-Exo. A. TEM observation of BMSC-Exo, the red arrow indicated exosomes; B. Protein bands of CD9, CD81, TSG101 and GRP94 detected by Western blot; C. Particle size and concentration of BMSC-Exo by ZateView detection.

6.6×10^{12} L^{-1} (Fig. 4C). The findings confirmed that BMSC-Exos were successfully isolated.

3.5. BMSC-Exos promote invasion and migration of lung cancer cells and lung metastasis in nude mice

To further explore the effect of BMSC-Exos on lung cancer, BMSCs-Exos were co-cultured with lung cancer cells A549 or NCI-H1299. After co-culture, a large number of red fluorescence-labeled BMSC-Exo were observed to be taken by lung cancer cells under the confocal microscope (Fig. 5A).

RT-qPCR and Western blot analysis showed that relative to the control group, CPEB1 expression decreased and miR-425 expression elevated in the BMSC-Exo group (all $P < 0.05$) (Fig. 5B and C).

Scratch test indicated that the BMSC-Exo group after 48-h scratching presented an increased distance versus the control group; by comparison with the BMSC-Exos group, the BMSC-Exos + GW4869 showed reduced scratch width (both $P < 0.05$) (Fig. 5D and E). Transwell assay exhibited that cell invasion ability was enhanced in the BMSC-Exo group versus the control group, while that was suppressed in the BMSC-Exo + GW4869 group versus the BMSC-Exos group (both $P < 0.05$) (Fig. 5F and G).

Lung metastasis model *in vivo* was established. HE staining suggested versus the control group, lung tissue metastasis was increased in the BMSC-Exos group ($P < 0.05$); with respect to the BMSC-Exos group, the BMSC-Exos + GW4869 group had reduced lung tissue metastatic lesions ($P < 0.05$) (Fig. 5H and I).

Analysis of N-cadherin and E-cadherin mRNA expression in lung tissues of nude mice presented that in comparison with the control group, N-cadherin mRNA expression increased and E-cadherin mRNA expression reduced in the BMSC-Exo group; versus the BMSC-Exos group, repressed N-cadherin and elevated E-cadherin mRNA expression was found in the BMSC-Exos + GW4869 group (all $P < 0.05$) (Fig. 5J).

3.6. Inhibitory effects of BMSC-Exos carrying down-regulated miR-425 or up-regulated CPEB1 on migration and invasion of lung cancer cells and lung metastasis in nude mice

To further explore whether BMSC-Exos can transmit miR-425 or CPEB1 to influence the invasion and metastasis of lung cancer cells and lung metastasis. The transfected BMSCs were co-cultured with A549 or NCI-H1299 cells. RT-qPCR and Western blot analysis suggested that miR-425 expression was decreased in the Exo-miR-425 inhibitor group, while CPEB1 expression had the opposite trend in relation to the Exo inhibitor-NC group ($P < 0.05$). Versus the Exo–pcDNA-NC group, the Exo-pcDNA-CPEB1 group showed no change in miR-425 expression ($P > 0.05$) and an increase in CPEB1 expression ($P < 0.05$). Versus the Exo-miR-425 mimic + pcDNA-NC group, there was no great change in miR-425 expression ($P > 0.05$), and a significant elevation in CPEB1 ($P < 0.05$) in the Exo-miR-425 mimic + pcDNA-CPEB1 group (Fig. 6A and B).

Scratch test and Transwell assay indicated that in relation to the Exo-inhibitor-NC group, Exo-pcDNA-NC group and Exo-miR-425 mimic + pcDNA-NC group, respectively, the Exo-miR-425 inhibitor group, Exo-pcDNA-CPEB1 group and Exo-miR-425 mimic + pcDNA-CPEB1 group manifested shortened wound healing distance and decreased migration ability (all $P < 0.05$) (Fig. 6C–F).

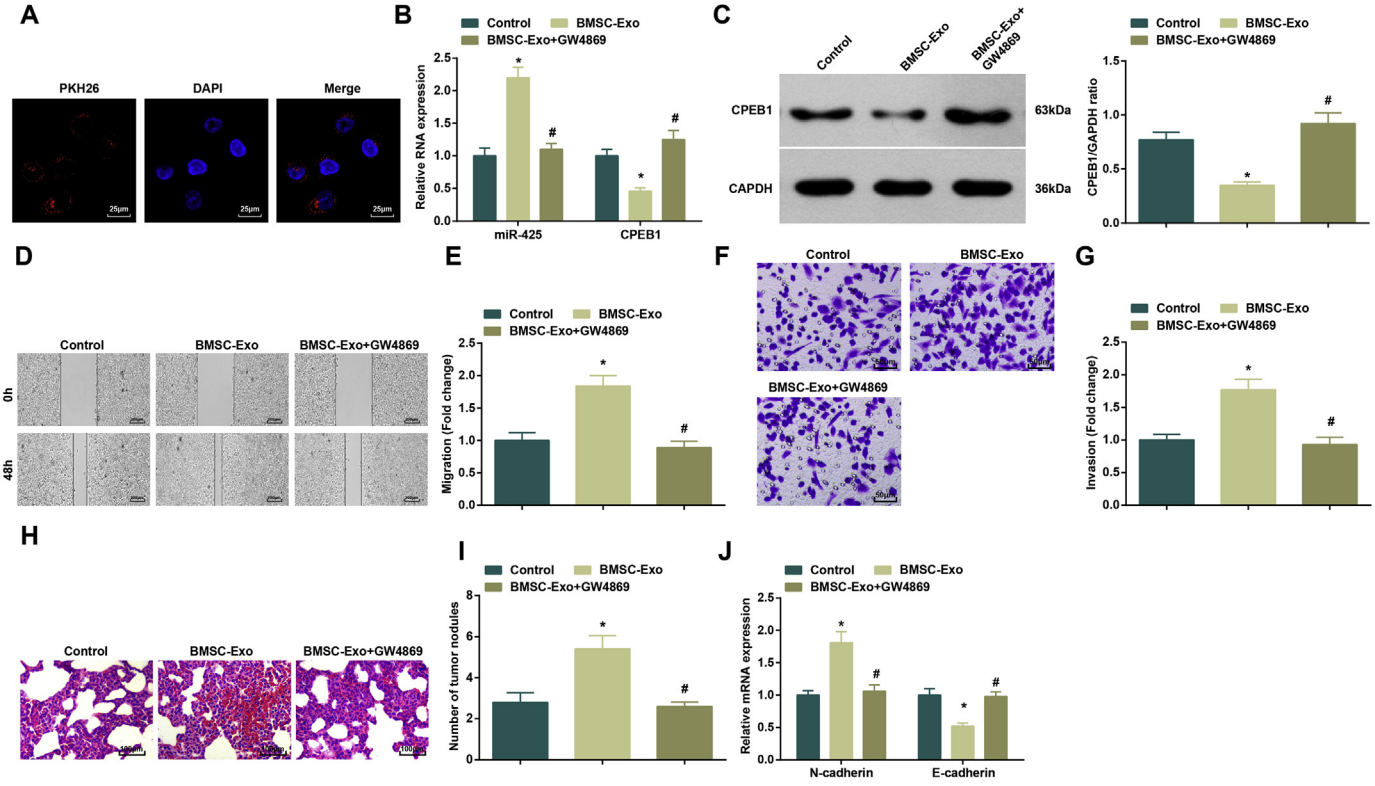

Fig. 5. BMSC-Exos promote migration and invasion of A549 cells and lung metastasis in nude mice. A. Observation of the uptake of BMSC-Exo by A549 cells with the confocal microscope; B. MiR-425 and CPEB1 mRNA expression in A549 cells after 24-h co-culture with BMSCs detected by RT-qPCR; C. CPEB protein expression in A549 cells after 24-h co-culture with BMSCs detected by Western blot analysis; D-E. Migration of A549 cells after 24-h co-culture with BMSCs detected by scratch test; F-G. Invasion of A549 cells after 24-h co-culture with BMSCs detected by Transwell assay; H. Observation of lung metastasis in nude mice by HE staining; I. The number of tumor nodules; J. N-cadherin and E-cadherin mRNA expression in lung tissues of nude mice. *$P < 0.05$ compared with the control group; #$P < 0.05$ compared with the BMSC-Exo group. Data were expressed as mean ± standard deviation.

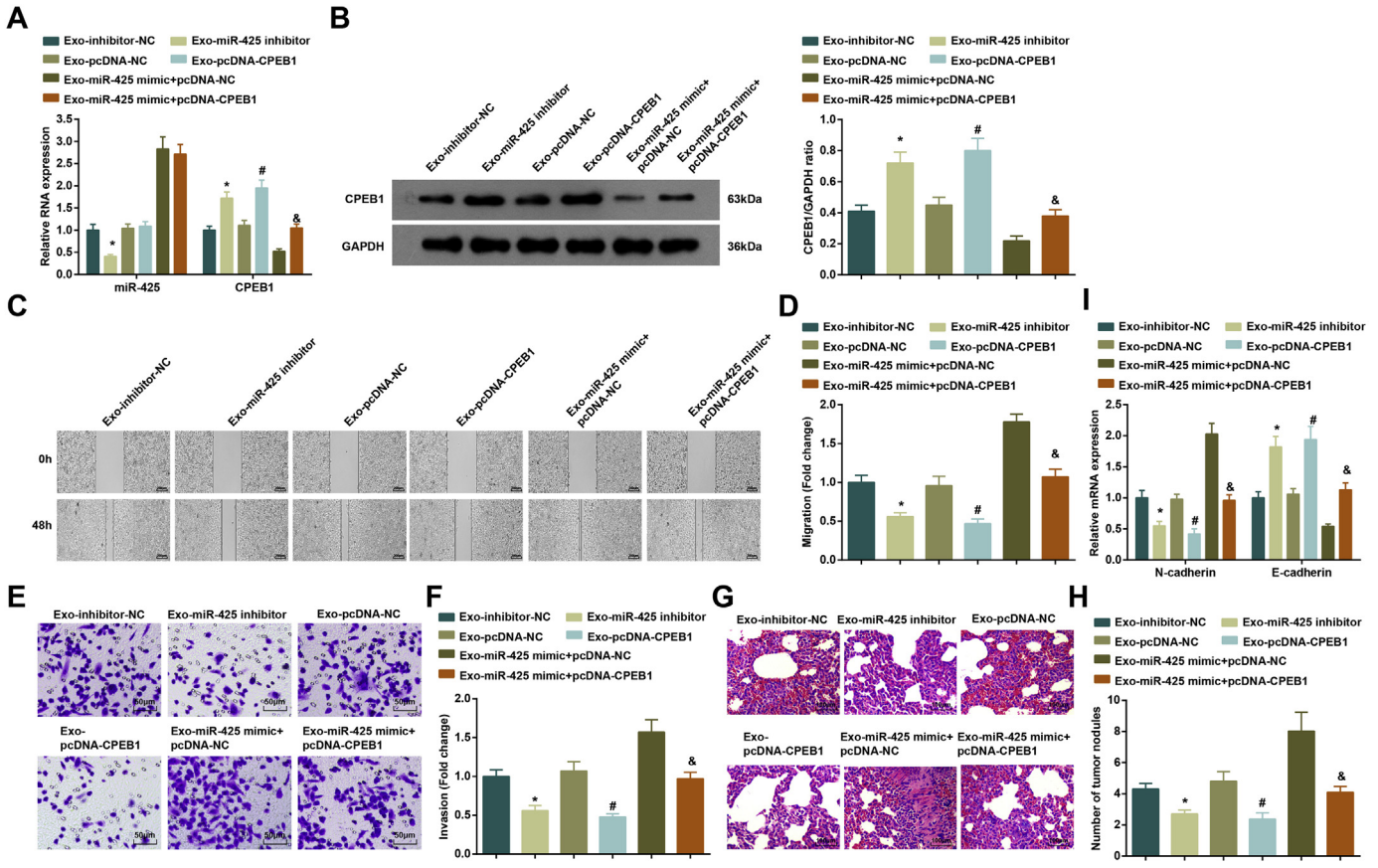

Fig. 6. Inhibitory effects of BMSC-Exos carrying down-regulated miR-425 or up-regulated CPEB1 on migration and invasion of A549 cells and lung metastasis in nude mice. A. MiR-425 and CPEB1 mRNA expression in A549 cells after 24-h co-culture with transfected BMSCs detected by RT-qPCR; B. CPEB1 protein expression in A549 cells after 24-h co-culture with transfected BMSCs detected by Western blot analysis; C-D. Migration of A549 cells after 24-h co-culture with transfected BMSCs detected by scratch test; E-F. Invasion of A549 cells after 24-h co-culture with transfected BMSCs detected Transwell assay; G. Observation of lung metastasis in nude mice by HE staining; H. The number of tumor nodules; I. N-cadherin and E-cadherin mRNA expression detected by RT-qPCR. *$P < 0.05$ compared with the Exo-inhibitor-NC group; #$P < 0.05$ compared with the Exo-pcDNA-NC group; & $P < 0.05$ compared with the Exo-miR-425 mimic + pcDNA-NC group. Data were expressed as mean ± standard deviation.

An *in vivo* lung metastasis model was constructed using A549 cells co-cultured with BMSCs after transfection. HE staining revealed nuclear distortion, nuclear pyogenic infection, nuclear fission and abnormal nuclear-cytoplasmic ratio in cells of lung tissues, and dense nuclear proliferation and void reduction on the tumor site in the Exo- inhibitor-NC group, Exo-pcDNA-NC group, Exo-miR-425 mimic + pcDNA-CPEB1 group and Exo-miR-425 mimic + pcDNA-NC group. The most tumor nodules were found in the Exo-miR-425 mimic + pcDNA-NC group. However, the tumor nodules in lung tissues reduced in the Exo-miR-425 inhibitor group and the Exo-pcDNA-CPEB1 group versus the Exo- inhibitor-NC group and the Exo-pcDNA-NC group (all $P < 0.05$) (Fig. 6G and H).

RT-qPCR highlighted that relative to the Exo-inhibitor-NC group, Exo-pcDNA-NC group and Exo-miR-425 mimic + pcDNA-NC group, N-cadherin mRNA expression reduced while E-cadherin mRNA expression elevated in the Exo-miR-425 inhibitor group, Exo-pcDNA-CPEB1 group and Exo-miR-425 mimic + pcDNA-CPEB1 group, respectively (all $P < 0.05$) (Fig. 6I).

4. Discussion

In recent years, although incidence and mortality rates of lung cancer have diminished as a result of a fall in cigarette use, it remains a malignancy at later stages with extremely poor survival [18]. Lately, evidence has shown that exosomes impact on the drug resistance of lung cancer cells [19]. Thus, our study was meant to explore how BMSC-Exos affect lung cancer cell progression by modulating miR-425 and CPEB1. Collectively, our study revealed that BMSC-Exos could deliver miR-425 to inhibit CPEB1 expression in lung cancer cells, thereby promoting the malignant biological properties of lung cancer cells and their metastasis *in vivo*.

As an essential part of cell-cell communication, exosomes could protect miRs from degradation and also deliver specific miRNAs from the supplier cells to the receiver cells [20]. A series of assays suggested that BMSC-Exos carrying up-regulated miR-425 or downregulated CPEB1 suppressed migration and invasion of lung cancer cells (A549 and NCI-H1299 cells) and lung metastasis (A549 cells) in nude mice. Similar to our study, a report has shown that 5T33 BMSC-Exos facilitate multiple myeloma cell progression and enhance drug resistance [6]. It is demonstrated that BMSC-Exos activate myeloid-derived suppressor cells in the bone marrow, resulting in boosted immunosuppression to assist multiple myeloma progression [21]. There has been a study proving that MSC-derived adipocyte exosomes can facilitate breast cancer cell growth [22]. According to a former paper, BMSC-Exos are found to promote colon cancer stem cell-like traits via miR-142-3p [23]. Besides, an update article has confirmed that BMSC-Exos could exert tumor promoter in the progression of osteosarcoma by transmitting miR-208a [23]. In addition to that, Xina Z et al. have proved that hypoxic BMSC-Exos could accelerate invasion of lung cancer cells through transfer of pro-tumor miRNAs, such as miR-193a-3p [24]. The aforesaid references imply that BMSC-Exos could deliver miRNA to exert functions in human diseases. As

reported, knockout of miR-425 in patients with acute respiratory distress syndrome serves as a master inducer of pulmonary fibrosis, which in return exacerbates lung injury [24]. Also, a latest study has implied the therapeutic effects of BMSC-Exos in acute myeloid leukemia through delivering miR-425-5p. Detailedly, inhibition of miR-425 in BMSCs delivered into the lung cells could reverse the protective role of BMSCs-Exos with the elevation of apoptosis rate, increase of Bax expression and reduction of Bcl-2 expression [25]. Therefore, miR-425 in BMSCs-Exos is conducive in attenuating lung cancer progression.

Other assays also indicated that CPEB1 was a direct target of miR-425, and miR-425 diminution elevated CPEB1 expression. The targeting relationship between CPEB1 and miR-425 has not been verified in the literature before. In addition, we found that underexpressed miR-425 or overexpressed CPEB1 restrained migration and invasion of lung cancer cells, and overexpressed CPEB1 reversed the contributory impacts of up-regulated miR-425 on migration and invasion of lung cancer cells. Consistent with the results, a previous study by Zhang X et al. has revealed that the elevation of miR-425 boosts breast cancer cell development while DICER1 silencing in the wake of the diminution of either miRNAs restrains the oncogenic behaviors [26]. Liu P et al. have demonstrated that miR-425 modulates IGF-1 to limits PI3K-Akt pathway, which further exerts negative impacts on melanoma metastasis [27]. There has been a research suggesting that miR-425-5p knockdown targets AIFM1 to restrict cervical cancer tumorigenesis [28]. It has been proposed that CPEB1 exerts suppressive impacts on cell stemness in hepatocellular carcinoma cancer [12]. There is also a report indicating that a drop in CPEB1 expression exerts contributory impacts on the lung metastasis of breast cancer cells *in vivo* [13]. A similar study illustrates that in endometrial cancer, elevated CPEB1 restrains cell development and tumor growth, and in return, a fall in CPEB1 expression induced by miR-183 facilitates EMT as well as migration and invasion of cancer cells [14]. These findings are in consistent with what we have obtained from a wide range of assays.

Taken together, our study reveals that human BMSC-Exos could deliver miR-425 to inhibit CPEB1 expression in lung cancer cells, thereby promoting the malignant biological properties of lung cancer cells and their metastasis *in vivo*. Our work offers new clues for the role of BMSC-Exos in lung cancer development and offers a new direction for clinical treatment of this disease through miR-425/CPEB1 axis. However, according to some prior studies, cancer-derived exosomes can promote breast cancer lung metastasis by delivering miRNA [29,30]. Also, cancer-derived exosomes can increase the metastatic ability of recipient cells, and promote lung cancer metastasis by delivering miRNA [31,32]. Furthermore, cancer-associated fibroblast-derived exosomes can affect cancer lung metastasis [33]. Therefore, whether other cell-type-derived Exos have similar effects on lung metastasis through miR-425 need in-depth exploration.

Declaration of competing interest

The authors have no conflicts of interest to declare that are relevant to the content of this article.

Acknowledgement

This Study was supported by Special project of Respiratory Clinical Medicine Research Center (Grant No.201912011)

Appendix A. Supplementary data

Supplementary data to this article can be found online at https://doi.org/10.1016/j.reth.2022.03.007.

Supplementary Figure 1Down-regulation of miR-425 or up-relation of CPEB1 inhibits NCI-H1299 cell invasion and migration. A. MiR-425 and CPEB1 mRNA expression in NCI-H1299 cells after transfection detected by RT-qPCR; B. CPEB1 protein expression in NCI-H1299 cells after transfection detected by Western blot; C-D. Migration of NCI-H1299 cells after transfection detected by scratch test; E-F. Invasion of NCI-H1299 cells after transfection detected by Transwell assay; $P < 0.05$ compared with the inhibitor-NC group; $\#P < 0.05$ compared with the pcDNA-NC group; & $P < 0.05$ compared with the miR-425 mimic + pcDNA-NC group. Data in the figure were expressed by mean ± standard deviation.

References

[1] Nasim F, Sabath BF, Eapen GA. Lung cancer. Med Clin 2019;103(3):463–73.
[2] Mao Y, Yang D, He J, Krasna M. Epidemiology of lung cancer. Surg Oncol Clin 2016;25(3):439–45.
[3] She J, Ping Y, Hong Q, Bai C. Lung cancer in China: challenges and interventions. Chest 2013;143(4):1117–26.
[4] Ostrowski M, Marjanski T, Rzyman W. Low-dose computed tomography screening reduces lung cancer mortality. Adv Med Sci 2018;63(2):230–6.
[5] Syn N, Wang L, Sethi G, Jean-Paul T, Boon-Cher G. Exosome-mediated metastasis: from epithelial-mesenchymal transition to escape from immunosurveillance. Trends Pharmacol Sci 2016;37(7):606–17.
[6] Wang J, Hendrix A, Hernot S, De Bruyne E, Van Valckenborgh E, Lahoutte T, et al. Bone marrow stromal cell-derived exosomes as communicators in drug resistance in multiple myeloma cells. Blood 2014;124(4):555–66.
[7] Chen L, Lu F, Chen D, Wu J, Hu E, Xu L, et al. BMSCs-derived miR-223-containing exosomes contribute to liver protection in experimental autoimmune hepatitis. Mol Immunol 2018;93:38–46.
[8] Liu R, Wang F, Guo Y, Yang Y, Chen S, Gao X, et al. MicroRNA-425 promotes the development of lung adenocarcinoma via targeting A disintegrin and metalloproteinases 9 (ADAM9). OncoTargets Ther 2018;11:4065–73.
[9] Yan YF, Gong F, Wang B, Zheng W. MiR-425-5p promotes tumor progression via modulation of CYLD in gastric cancer. Eur Rev Med Pharmacol Sci 2017;21(9):2130–6.
[10] Fang F, Song T, Zhang T, Cui Y, Zhang G. MiR-425-5p promotes invasion and metastasis of hepatocellular carcinoma cells through SCAI-mediated dysregulation of multiple signaling pathways. Oncotarget 2017;8(19):31745–57.
[11] Zhang X, Sai B, Wang F, Wang L, Zheng L, Li G, et al. Hypoxic BMSC-derived exosomal miRNAs promote metastasis of lung cancer cells via STAT3-induced EMT. Mol Cancer 2019;18(1):40.
[12] Xu M, Fang S, Song J, Chen M, Zhang Q, Weng Q, et al. CPEB1 mediates hepatocellular carcinoma cancer stemness and chemoresistance. Cell Death Dis 2018;9(10):957.
[13] Nagaoka K, Fujii K, Zhang H, Usuda K, Watanabe G, Ivshina M, et al. CPEB1 mediates epithelial-to-mesenchyme transition and breast cancer metastasis. Oncogene 2016;35(22):2893–901.
[14] Xiong H, Chen R, Liu S, Lin Q, Hui C, Jiang Q. MicroRNA-183 induces epithelial-mesenchymal transition and promotes endometrial cancer cell migration and invasion in by targeting CPEB1. J Cell Biochem 2018;119(10):8123–37.
[15] Deng Q, Fang Q, Xie B, Sun H, Bao Y, Zhou S. Exosomal long non-coding RNA MSTRG.292666.16 is associated with osimertinib (AZD9291) resistance in non-small cell lung cancer. Aging (N Y) 2020;12(9):8001–15.
[16] Xu S, Zheng L, Kang L, Xu H, Gao L. microRNA-let-7e in serum-derived exosomes inhibits the metastasis of non-small-cell lung cancer in a SUV39H2/LSD1/CDH1-dependent manner. Cancer Gene Ther; 2020.
[17] Zhang N, Nan A, Chen L, Li X, Jiang Y. Circular RNA circSATB2 promotes progression of non-small cell lung cancer cells. Mol Cancer 2020;19(1):101.
[18] Schwartz AG, Cote ML. Epidemiology of lung cancer. Adv Exp Med Biol 2016;893:21–41.
[19] Xia X, Yu S, Li S, Wu J, Rong M, Cao H. Exosomes: decreased sensitivity of lung cancer A549 cells to cisplatin. PLoS One 2014;9(2):e89534.
[20] Park HJ, Bach DH, Lee SK, Hong JY. The role of exosomes and miRNAs in drug-resistance of cancer cells. Int J Cancer 2017;141(2):220–30.
[21] Wang J, De Veirman K, De Beule N, Maes K, De Bruyne E, Van Valckenborgh E, et al. The bone marrow microenvironment enhances multiple myeloma progression by exosome-mediated activation of myeloid-derived suppressor cells. Oncotarget 2015;6(41):43992–4004.
[22] Wang S, Su X, Xu M, Xiao X, Li X, Li H. Exosomes secreted by mesenchymal stromal/stem cell-derived adipocytes promote breast cancer cell growth via activation of Hippo signaling pathway. Stem Cell Res Ther 2019;10(1):117.
[23] Li H, Li F. Exosomes from BM-MSCs increase the population of CSCs via transfer of miR-142-3p. Br J Cancer 2018;119(6):744–55.
[24] Wang L, Liu J, Xie W, Li G, Zhang R, Xu B. miR-425 reduction causes aberrant proliferation and collagen synthesis through modulating TGF-beta/Smad signaling in acute respiratory distress syndrome. Int J Clin Exp Pathol 2019;12(7):2604–12.
[25] Zhang L, Khadka B, Wu J, Feng Y, Long B, Xiao R, et al. Bone marrow mesenchymal stem cells-derived exosomal miR-425-5p inhibits acute

myeloid leukemia cell proliferation, apoptosis, invasion and migration by targeting WTAP. OncoTargets Ther 2021;14:4901–14.
[26] Xiao Z, Wu M, Chong Q, Zhang W, Qian P, Hong Y, et al. Amplification of hsa-miR-191/425 locus promotes breast cancer proliferation and metastasis by targeting DICER1. Carcinogenesis 2018;39(12):1506–16.
[27] Liu P, Hu Y, Ma L, Du M, Xia L, Hu Z. miR-425 inhibits melanoma metastasis through repression of PI3K-Akt pathway by targeting IGF-1. Biomed Pharmacother 2015;75:51–7.
[28] Zhang Y, Yang Y, Liu R, Meng Y, Tian G, Cao Q. Downregulation of microRNA-425-5p suppresses cervical cancer tumorigenesis by targeting AIFM1. Exp Ther Med 2019;17(5):4032–8.
[29] Xun J, Du L, Gao R, Shen L, Wang D, Kang L, et al. Cancer-derived exosomal miR-138-5p modulates polarization of tumor-associated macrophages through inhibition of KDM6B. Theranostics 2021;11(14):6847–59.
[30] Delcayre A, Shu H, Le Pecq JB. Dendritic cell-derived exosomes in cancer immunotherapy: exploiting nature's antigen delivery pathway. Expert Rev Anticancer Ther 2005;5(3):537–47.
[31] Ichikawa H, Suetsugu A, Satake T, Aoki H, Hoffman RM. Exosome transfer between pancreatic-cancer cells is associated with metastasis in a nude-mouse model. Anticancer Res 2021;41(6):2829–34.
[32] Nie H, Xie X, Zhang D, Zhou Y, Jia L. Use of lung-specific exosomes for miRNA-126 delivery in non-small cell lung cancer. Nanoscale 2020;12(2):877–87.
[33] Zhang Y, Zhao J, Ding M, Su Y, Han B. Loss of exosomal miR-146a-5p from cancer-associated fibroblasts after androgen deprivation therapy contributes to prostate cancer metastasis. J Exp Clin Cancer Res 2020;39(1):282.